The analysis of H/V curve from different ellipticity retrieval technique for a single 3c-station recording.

3 Irfan Ullah[1], Renato Luiz Prado[1].

4 1.Departamento de Geofísica do Instituto de Astronomia, Geofísica e Ciências Atmosféricas

5 Rua do Matão, 1226 - Cidade Universitária São Paulo-SP - Brasil

6 *Correspondence to*: Irfan Ullah (syed_528@yahoo.com)

7 **Abstract.** In the last two decades or so the H/V (Horizontal-to-Vertical Spectral Ratio) technique remained very popular,

8 and are extensively used for the site fundamental frequency estimation. H/V curve also used with dispersion curve to

9 jointly invert and retrieved the shear wave velocity of relatively deep soil deposit. Although a full theoretical explanation of

10 H/V technique is not been presented yet, There are two main assumptions used generally that H/V curves can be explained

11 by considering Rayleigh wave of noise wave field only while the other newly presented approach utilizes the whole noise

12 wave field known as diffuse field approach (DFA). However in case of Rayleigh wave approach for H/V, it is almost

13 impossible to the remove the fraction of Love wave the horizontal component of H/V. Here in this study we aim to test

14 different approaches adopted for the removal of Love wave fraction from horizontal component for a borehole test site at

15 University of Sao Paulo. The result from different approaches are compared with borehole ellipticity curve. The result

16 shows that around the fundamental frequency of wave obtained in either way(DFA or ellipticity approach) is dominated by
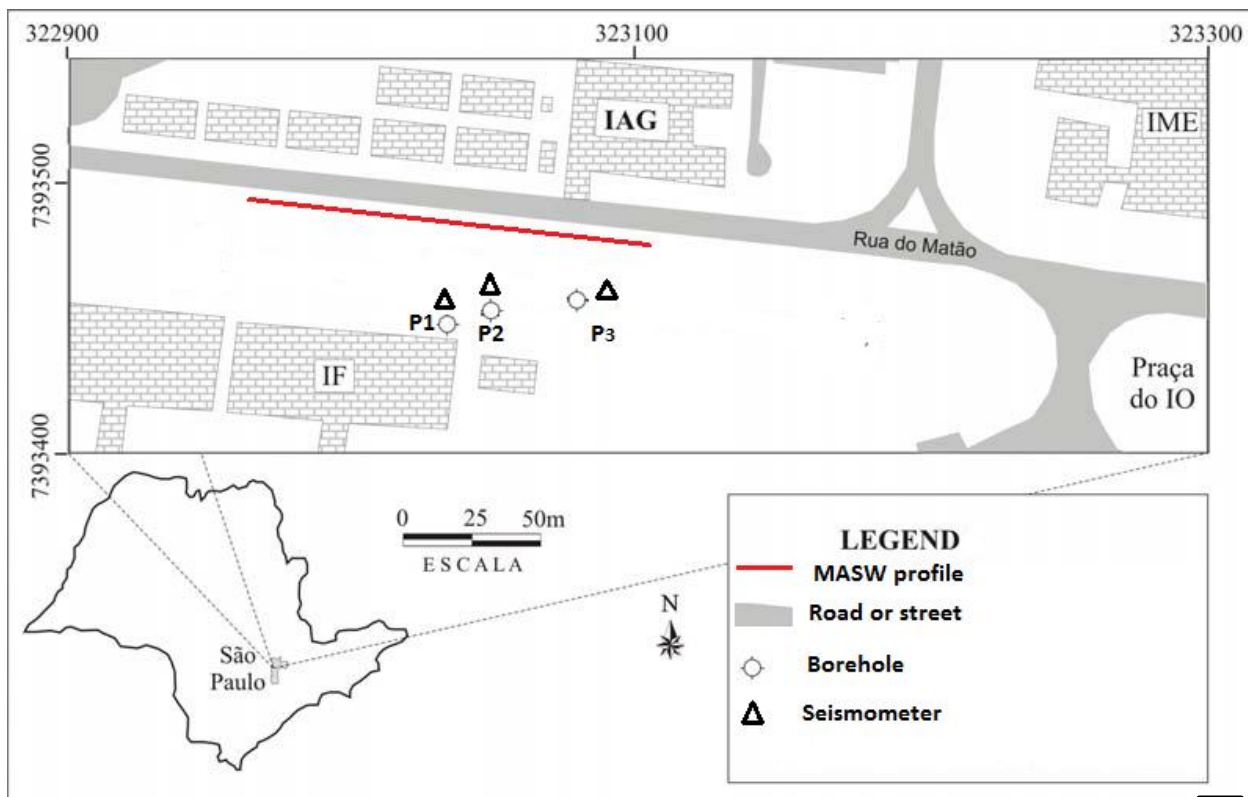
17 Rayleigh waves.

18

1. Introduction.

20

21 H/V (Horizontal-to-Vertical spectral ratio) is fast and quick way to get properties of a site for

22 engineering interest, by the measurement of ambient noise wave field with a single 3-component sensor

23 on the earth surface. The method is used for rapid estimation of fundamental resonance frequency (f_0)

24 of a site where the maximum displacement amplification is expected in case of an earthquake. This

25 technique is also used to retrieve the shear wave velocity of the geological structure in a joint inversion

26 with dispersion curve (Scherbaum et al, 2003 Picozi et al, 2005 Hobiger et al, 2013). However, some

27 controversies about the nature of ambient noise wave field and sources exist, which most of the time

28 make the results of H/V curve questionable and hence debatable. Apart from the controversies exist in

29 nature of ambient noise wave filed M. Mucciarelli et al (2001) described some problem regarding the

Natural Hazards
and Earth System
Sciences
Discussions

Open Access

EGU

30 acquisition and processing of H/V spectral ratio. Due to extensive utilization of H/V technique, a

31 commission was established to test the acquisition, processing and interpretation of this technique (site

32 effects assessment using ambient excitations) – the SESAME project (2001-2004), The guidelines

33 reports are published for acquisition, processing and interpretation of ambient noise wave field and have

34 addressed all the points raised and discussed by M. Mucciarelli et al (2001) in extensive details. The

35 H/V curve a modeled with different approaches and each modeling approach might have the effect on

36 the retrieved soil profile(Sánchez-Sesma et al, 2011, Lunedei & Malischewsky 2015 the acquisition

37 of the data is made with a three component sensor placed on the surface of ground which record the

38 seismic noise wave field. Fourier spectra of the recorded seismic noise for all the three component (eat-

39 west , north-south and vertical) are ma The two horizontal component Fourier spectra are properly

40 averaged and then divided by the vertical Fourier spectra. This division of averaged horizontal and

41 vertical component result a curve (H/V) as function of frequency. H/V curve usually result a peak

42 depending on the subsoil stratigraphical profile, this peak correspond to fundamental resonance

43 frequency (f_0) of the site (Tokimatsu, 1997; Bard, 1999; Bonnefoy-Claudet et al., 2006). The averaged

44 horizontal component of H/V curve contai he contribution from both Rayleigh and Love wave and

45 some fraction of body waves as well. In a joint inversion of H/V curve with dispersion curve this other

46 elastic wave effect presence in the H/V curve might bias the retrieved s-wave velocity profile.

47 Therefore, the presence of Love and other elastic waves existence in the H/V curve must be assumed or

48 estimated before the inversion process (Bonnefoy-Claudet et al., 2006).Here in this communication we

49 will try to list the different approaches used for the refining H/V curve by removing unwanted

50 fraction (Love wave effect presence) prior to the joint inversion with dispersion curve. At present there

51 are two main research lines describing the H/V curve by taking in account the whole ambient-vibration

52 wave field, and another just studies the surface wave and Rayleigh wave dominancy in noise wave field

53 (Lunedei & Malischewsky 2015). Sánchez-Sesma et al (2011) proposed that seismic noise field can be

54 consider as diffusion-like situation which contain all type of elastic wave (surface and body waves) . He

55 suggested that the average autocorrelation of the motions at a given receiver, in the frequency domain,

56 measures average energy density (DED) and is proportional to the imaginary part of the Green function

57 (GF) when both source and receiver are the same. The surface wave dominancy opinion of noise wave

Natural Hazards
and Earth System
Sciences

Discussions

58 field is in favor of Rayleigh wave dominancy (Yamamoto, 2000 Boremann 2002, Cornou, 2002 ,

59 Okada ,2003). We will try to check both these assumptions here with the borehole data.

60 The site for which this analysis are made is a borehole site at university of Sao Paulo shown in Fig.1.

61 The noise measurement were made with broadband 3 component seismometer nanometrics Trillium

62 Compact 120-s. Ambient noise wave field measurements were made for 24 hours on weekend night to

63 minimized cultural noise influence. The data acquisition of ambient noise has been done following the

64 guidelines developed under the SESAME (2004) recommendations. To obtain the fundamental

65 frequency of the site a window of one-hour recording were processed and the reliability condition

66 proposed by SESAME (2004) for the H/V curve and peak were followed.

68 Fig. 1 shows the location map studied area ,legends explain the different symbols. (modified from Porsani 2004.)

69 We will try to discuss briefly here and analyzed our seismic noise data with this diffuse-field

70 assumption (DFA). Later we will analyzed our data with assumption that H/V curve basically reflect the

71 Rayleigh wave ellipticity.

73 **2. Diffuse field assumption technique.**

Natural Hazards
and Earth System
Sciences
Discussions

74

75 Sánchez-Sesma et al (201) proposed to considered ambient noise wave field as diffuse wave field

76 which contain all different types of waves (surface and body). The ambient noise wave field is

77 generated by multiple random uncorrelated forces/sources near to or at the earth surface. The wave

78 field may contain the scattering effect of various elastic mode. The field intensities could be in a better

79 way described by diffuse like situation. To assume that the noise wave field is diffuse, the H/V curve

80 can be estimated for a receiver at earth surface in term of green tensor imaginary part at the source

81 (source and receiver are assumed to be at same location). The work of Sánchez-Sesma provides an idea

82 of linkage between energy density and imaginary part of GF in 3D (energy densities of the noise wave

83 field is proportional to the imaginary part of green tensor). The H/V curve obtained from the square

84 root ratio of imaginary parts of GF (horizontal and vertical components) Eq.2 serve as intrinsic

85 property of medium therefore its inversion can be used to retrieved subsurface soil profile. The detailed

86 analysis of the method is beyond the scope of this ~~communique~~ nterested readers are referred to

87 Sánchez-Sesma et al (2011) for ~~detailed proce~~ ure. The summary of this procedure is that

88 autocorrelation of motion at a receiver sensor in a given direction is proportional to directional energy

89 density (DED),and this DED is proportional to the imaginary part of Green tensor at that sensor

90 (Sánchez-Sesma et al 2011). Patro al,(2009) showed that in case of 3D homogeneous elastic half

91 space, the horizontal displacement (radial and transverse) have fix energy proportion (e.g $E_1(x,x,\omega) =$

92 $E_2(x,x,\omega)$ and also $ImG_{11}(x,x,\omega) = ImG_{22}(x,x,\omega)$). For a diffused wave field the H/V can be

93 represented in term of directional energy densities assuming source and receiver lies at same location

94 (x) on the surface of earth as

95

96 $\frac{H}{V}(\omega) = \sqrt{\left(\frac{E_1(x,x,\omega)+E_2(x,x,\omega)}{E_3(x,x,\omega)}\right)}$ (1)

97

98 $\frac{H}{V}(\omega) = \sqrt{\left(\frac{ImG_{11}(x,x,\omega)+ImG_{22}(x,x,\omega)}{ImG_{33}(x,x,\omega)}\right)}$ (2)

99 where in (1)

$E_m(x,\omega) = \rho\omega^2\langle u_m(x,\omega)u_m^*(x,\omega)\rangle$ where m $= 1,2,3$
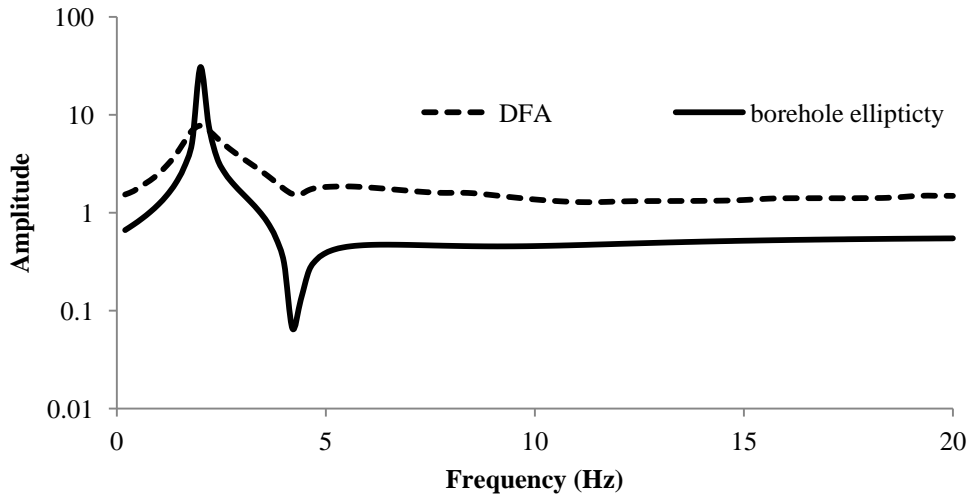
100

$= -2\pi\mu E_s k_s^{-1} Im[G_{mm}(x,x,\omega)]$

101

102 where energy density is find out at point x in direction m. ω, ρ and u_m are angular frequency , layer

103 density and displacement at point x respectively . $E_s = \rho\omega^2 s^2$ is the strength of diffuse illumination in

104 term of shear wave average energy density μ is shear wave modulus $\langle...\rangle$ bracket shows the azimuthal

105 average, $k_s = \frac{\omega}{V_s}$ shear wave number V_s shows medium S-wave velocity. The symbol $(.^*)$ show complex

106 conjugate process, the medium response in a direction m (of impulse load and acting in same direction)

107 is indicated by G_{mm} .The H/V curve obtained in this manner a□nked to the intrinsic property of

108 medium , The resulted H/V curve from the diffuse-field approach might allow its inversion without

109 considering any supplemented information (dispersion curve).

110

111 For our analysis, the data of seismic noise recorded at borehole test site were analyzed with DFA

112 (diffuse field assumption) frame work of Eq.2 , $\frac{H}{V}(\omega)$ resu□re obtained from the data with an

113 integration step of 1000 and window length 40s.The curve obtained by this directional energy density

114 approach is compared with borehole ellipticity Fig.2. The peak and trough of H/V curve obtained

115 (Fig.2) correspond to peak and trough of ellipticity. However the shape of H/V curve is generally higher

116 except the peak ,~~it is~~ because of other elastic wave phases contribution. This peak and trough

117 correlation of the H/V curve with borehole ellipticity shows that at these singularities (peak and trough)

118 Rayleigh wave contribution dominate the wave-field. It is important to note here the inversion of

119 ellipticity curve with dispersion curve are recommended around the peak region of H/V curve (Picozi

120 et al,2005 Hobiger et al, 2013). In next section we will focus our attention on the other line of research

121 which is in the opinion of, that noise wave field is dominated by surface wave especially Rayleigh

122 wave (see section 3) , and H/V curve can be explained by its correlation with Rayleigh wave ellipticity

123 curve (Bard 1999).

124

Fig.2 H/V curve obtained through DFA technique at the test site (IAG-USP), the Borehole ellipticity curve is plotted in solid for comparison at the site.
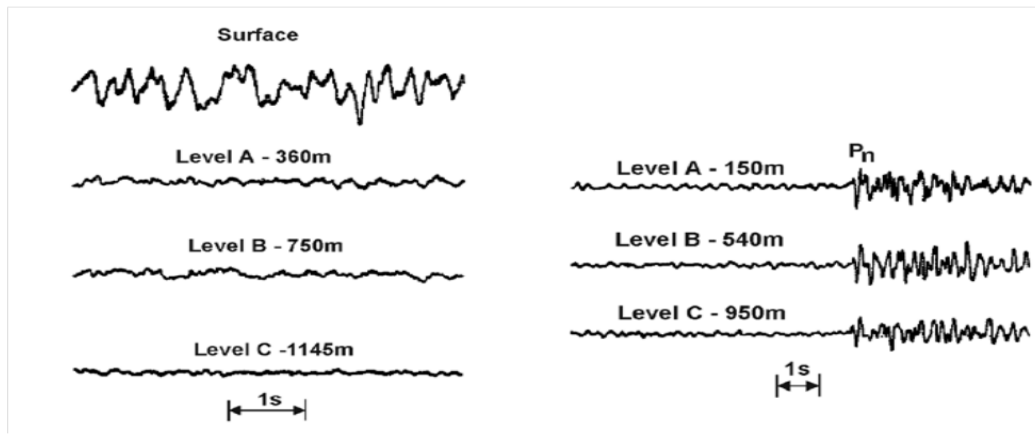
3. Surface wave dominancy of seismic noise wave field.
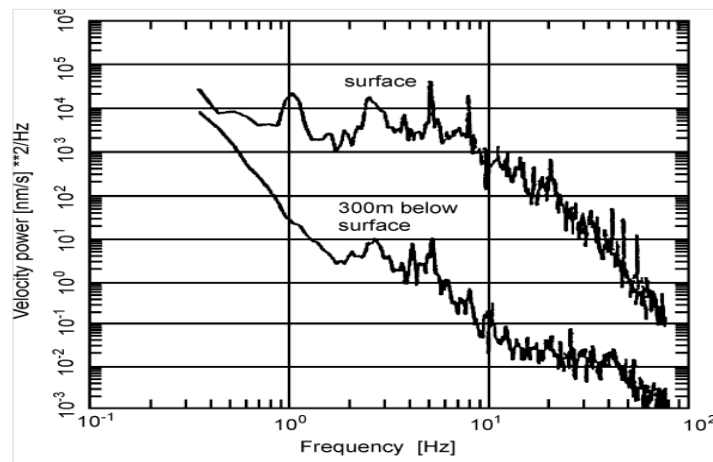
To find out that whether body or surface waves dominate the noise wave field is analyzed by Bormann (2002) , housed sensors for earthquake and seismic noise recording both at the surface and in the boreholes at different depth levels and concluded the surface-wave nature of seismic noise Fig. 3. Bormann (2002) showed that, the penetration depth of surface waves increases with wavelength, high frequency noise attenuates more rapidly with depth. In case of Fig.3 the noise power at 300 m depth in a borehole was reduced, as compared to the surface, by about 10 dB, at f = 0.5 Hz, 20 dB at 1 Hz and 35 dB at 10 Hz. This continuous amplitude decline with frequency is in accord with the surface waves nature of seismic noise.

6

141

142 Fig.3 Recording of seismic noise (left) and earthquake signals (right) at the surface and at different depth levels of a

143 borehole. (Bormann 2002).

144

145 Fig. 4 Velocity power density spectra as obtained for noise records at the surface (top) and at 300 m depth in a borehole

146 (below) near Gorleben, Germany (Bormann , 2002).

147 If the noise wave field is mainly dominated by surface wave then another question arises that what is

148 the fraction contribution of Rayleigh and Love waves to the noise wave field. Most of the researchers

149 focused their attention to find the fraction Rayleigh to Love ratio from the analysis of noise wave field

150 recorded on vertical component (Li et al., 1984; Horike, 1985; Yamanaka et al., 1994). The results of

151 these studies showed an agreement in one aspect that microseism ($<1Hz$) are mainly dominated by

152 Rayleigh waves however at high frequency ($>1Hz$) a combination of P and Rayleigh wave exists
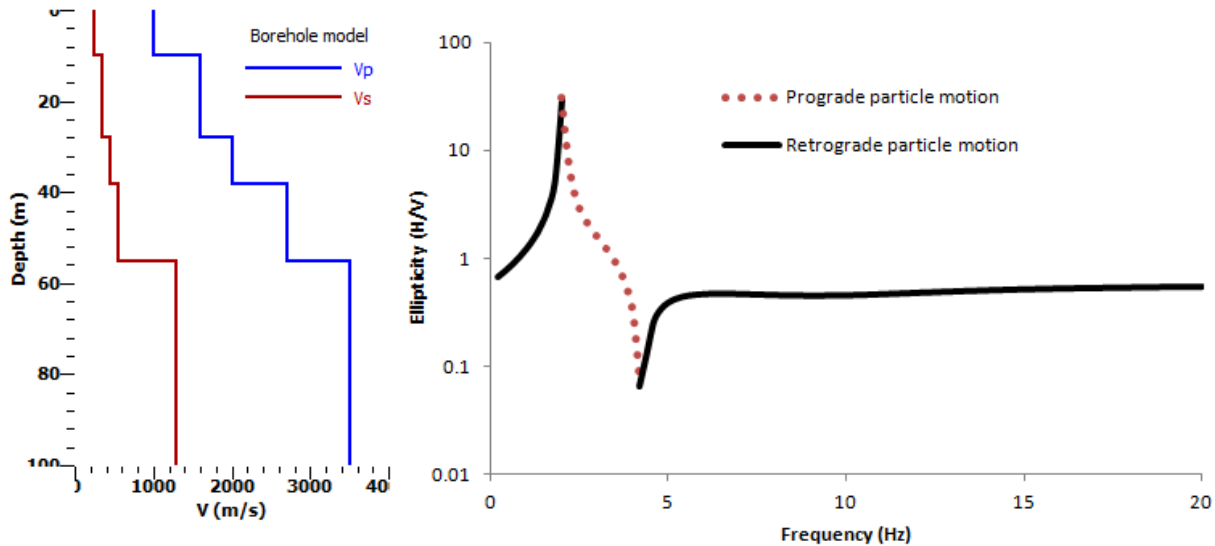
153

154 Table 1 summarize the result of previous studies on this issue.

Natural Hazards
and Earth System
Sciences
Discussions

	Rayleigh waves(%)	Love waves(%)	frequency range(%)
Chouet et al.,1998	30%	70%	>2Hz
Yamamoto, 2000	<50%	>50%	3-10 Hz
Arai et al., 1998	30%	70%	1-12 Hz
Cornou, 2002	60%	40%	< 1 Hz
Okada (2003)	<50%	>=50%	0.4-1 HZ
Köhler(2006)	10–35%	65–90%	0.5–1.3 Hz

155

156 Table.1 Summary conclusions about the proportion of Rayleigh and Love waves in noise, after different authors (from
157 Chouet et al., 1998; Yamamoto, 2000; Arai et al. 1998; Cornou 2002, Okada 2003, Köhler2006)

158 **4.Removal of Love wave from horizontal component.**

159 Rayleigh waves are formed by the linear pairing of P (primary waves) and Sv (vertically polarized
160 shear waves) waves (Aki, 2002).This pairing of vertical and horizontal components have a phase shift
161 of $\pm\frac{\pi}{2}$, the particle motion induced by Rayleigh wave will dipict an ellipse, the elliptical motion will
162 either be retrograde or prograde depending on the sign of phase shift. Similarly Love waves composed
163 of horizontally polarized shear waves (SH) The horizontal over vertical axes of ellipse described by
164 particle motion under the Rayleigh wave influence is terms ellipticity. At situation of homogeneous
165 half-space the particle motion is retrograde at all frequencies and ellipticity is constant . However in
166 case of layered structure ellipticity exhibit a peak and trough and the particle motion switch from
167 retrograde to prograde and then to retrograde with the frequency, depending on the velocity contrast
168 between the soil and bedrock (Konno and Ohmachi, 1998).

Fig.5 Borehole model at IAG-USP . The ellipticty curve of fundamental Rayleigh wave of the borehole model , marking the frequency ranges where the retrograde and prograde motion might occur.
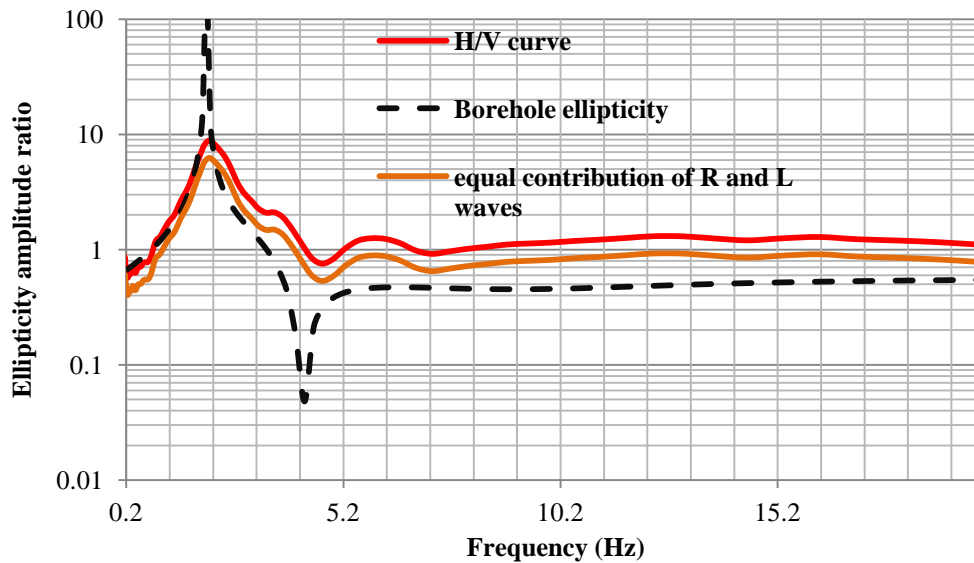
The conclusion from the preceding section can be drawn that, the contribution of Love wave to the horizontal is not predictable and fluctuate with frequency and from site to site. The H/V linked to the ellipticity of Rayleigh wave , in situation where ~~the~~ high shear wave contrast exist between soil and bedrock (Bard,1999).The H/V curve corresponds nicely to the peak of ellipticity curve (Fig.6). The deviation between curves can be easily linked to the presence of Love wave contribution to noise wave field at the horizontal component. We will try to review all the available technique for the this task and compared its result with borehole ellipticity.

H/V curves are obtained and compared with the elliptiity curve of borehole at the same site. The deviation between the curves are due to Love wave contribution. H/V curve is generally higher than the ellipticity curve except at peak frequency of Rayleigh wave ellipticity Fig.6. Three different polarization technique re used to minimized the effect of Love wave. The first technique is the simple H/V of seismic noise (Fig.6) , In this technique the polarization mean the division of Fourier spectral amplitude of averaged horizontal component over vertical component with the assumption that around the fundamental resonance frequency the vertical component is dominated by Rayleigh only. Generally it is

188 believed that Rayleigh (P-SV) and Love wave (SL) contribute equally to the horizontal component. Fäh

189 et al (2001) proposed the division of H/V spectral amplitude by $\sqrt{2}$ for Love wave effect minimization

190 from horizontal component Fig.6. However this is not a wise approach because the energy partition of

191 horizontal component between Rayleigh and Love is not constant and varies with frequency and site

192 (Köhler *et al.* 2006; Endrun 2011) Table There are two other polarization approaches employed for

193 this job recently ~~are~~: time-frequency analysis (Fah et,al 2009) and RayDec (Hobiger et, al, 2009)

194 ~~followed by a concise introduction , the interested readers are referred for detail of these approaches~~

195 ~~(Fah et,al 2009) and (Hobiger 2009).~~

196

197 Fig.6 shows the comparison of H/V curve of experimental data recorded at test borehole site at university of Sao Paulo.

198

5. Time-frequency analysis.

200

201 In time-frequency analysis the vertical component of noise wave field a considered as a trigger and its

202 energy level are estimated at given time and frequency and ~~are~~ correlated with horizontal components

203 (east-west , and north- south). A brief description of the technique is that continuous wavelet

204 transformation (CWT) are performed on the east~~ern~~ e(t) , north~~ern~~ n(t) and vertical v(t) components of

205 noise wave field. CWT ~~(continuous wavelet transform)~~ transform a signal to time-scale plane. The

206 scale is a single parameter which controls both the duration and bandwidth.CWT is defined as.
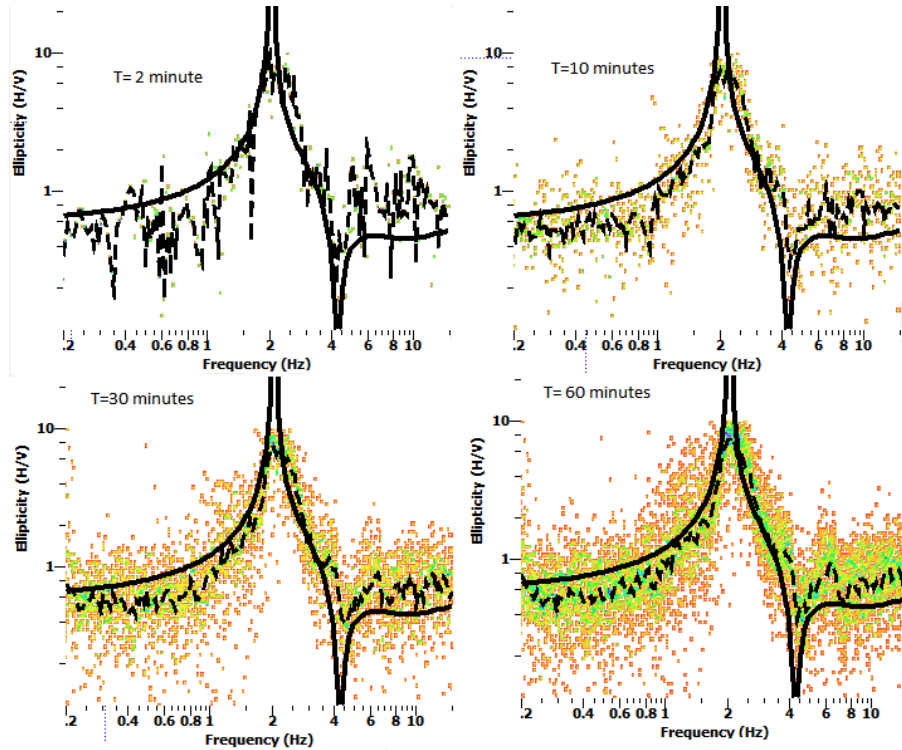
207 $CWT_{x(t)}(a, b) = \frac{1}{\sqrt{a}} \int_{-\infty}^{\infty} x(t) \psi^* \left(\frac{a-b}{a} \right) dt$ (3)

208 where x(t) is real-valued signal component {where x(t) = e(t) or n(t) or v(t) }, *ψ(t) shows the mother*

209 *wavelet,** shows a complex conjugation process, a scale parameter (scale control both the duration and

210 bandwidth) b is translation in time. Fah et,al (2009) used a modified Morelet wavelet in a code written

211 for this job due the reason that traditional Morelet wavelet does not act well for H/V analysis. The

212 modified Morelet transform is defined as

213 $\psi(t) = \exp{(i2\pi ft)} e^{\left(\frac{-t^2}{m} \right)}$ (4)
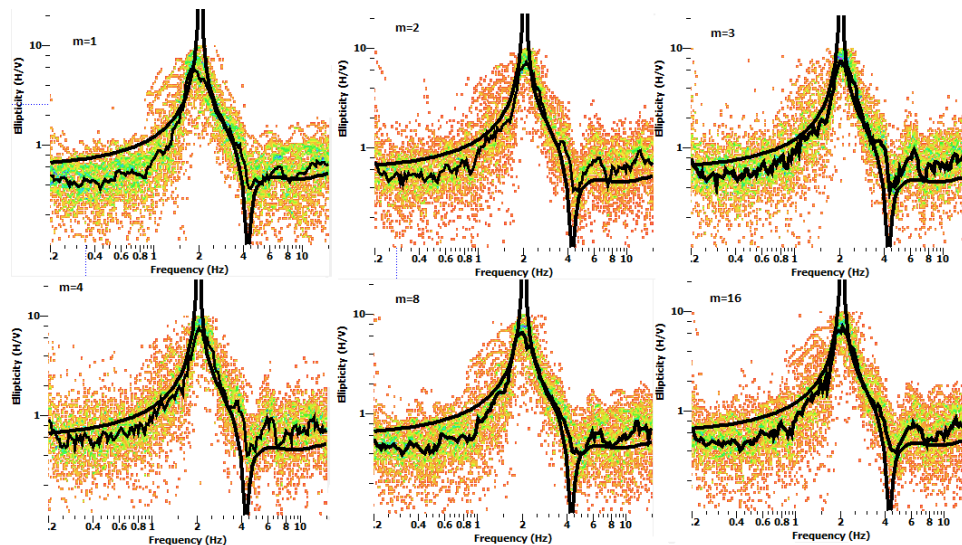
214 here f is the central frequency of the wavelet, m control the resolution of both frequency and time, low

215 m mean more time localization on the expense of frequency resolution and higher m result on the

216 contrary i.e increase frequency resolution at the expense of time resolution. The classical Morelet

217 wavelet is achieved when m=1/2. After the application of CWT to each component of a single 3-c

218 sensor recording { e(t), n(t) or v(t) } give rise to three signals amplitude which is both the function of

219 time and frequency. Two horizontal (e(t), n(t)) component are merged together to a single component.

220 As Rayleigh wave are the result of the coupling of p and vertically polarized S-waves, The vertical

221 component is sorted out for amplitude maxima at each frequency and time translation . Similarly, the

222 horizontal component is analyzed for amplitude maximum at given frequency and time, the horizontal

223 components are phase shifted ± at a quarter of the period. This shift of period is done because of

224 theoretical phase shift between $\pm\frac{\pi}{2}$ vertical and horizontal component particle motion. For each

225 maximum on the vertical component, the corresponding maximum on the horizontal component are

226 stored and the ratio of H/V are estimated. There is only one tuning parameter m ,the effect of it

227 different values of m are shown in Fig.8 ,Also the effect on the length of the recorded signal is shown

228 in Fig.7. This whole process is statistically analyzed by histogram for all the frequency and translation

229 of time and H/V is obtained by the maximum of each histogram. For de theoretical outline of this

230 analysis please read (Fah et,al, 2009).

11

231

Fig.7 Ellipticity (H/V) obtained from continuous wavelet transformation CWT for different length of the recorded signal; a

histogram is drawn for each frequency, the color within histogram indicates the energy level. (dashed line shows ellipticity

obtained from CWT while solid line shows the ellipticity curve obtained from borehole data at same location - IAG-front)

235

236

Natural Hazards
and Earth System
Sciences
Discussions

237

Fig.8 Ellipticity (H/V) obtained from continuous wavelet transformation CWT for different value of m; (curvy line shows ellipticity obtained from CWT while solid line shows the ellipticity curve obtained from borehole data at same location - IAG-front)

241

Fig.7 and 8 show a better result when compared with the borehole ellipticity curve of borehole. The result of wavelet transform Fig.7&8 shows that the ellipticity of borehole is retrieved in better way(especially at right limb of the ellipticity) when the recorded length of the signal is greater than 30 minute ,and when the value of m ≥ 8.

246

6 Random decrement technique (RAYDEC).
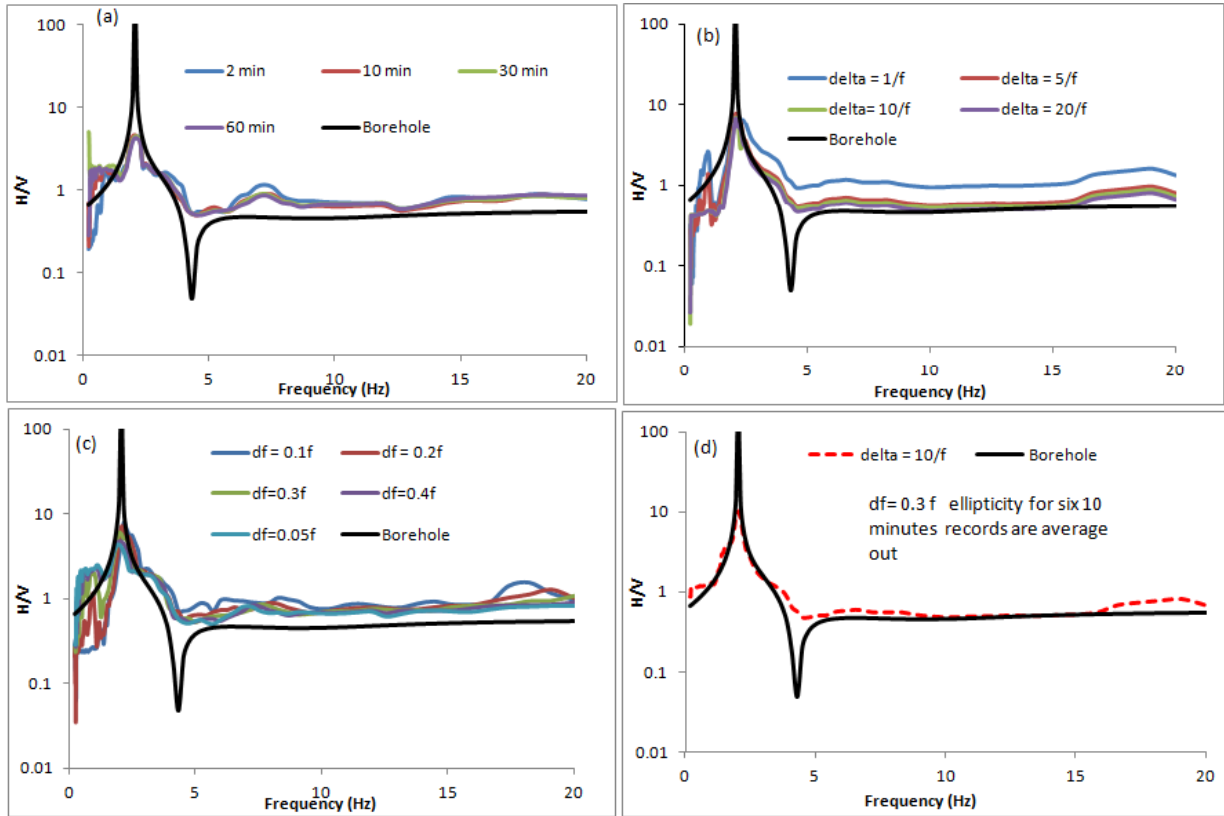
Another polarization technique use for the effect of Love (Sh) wave effect minimization for a single 3 component sensor recording is term as RayDec technique (Hobiger et.al, 2009) The vertical component is taken as master trigger as because the S arrival occur only on the vertical component, while stacking a large number of horizontal component to obtained ellipticity of Rayleigh curve (Hobiger et al., 2009) showed that the obtained ellipticity will be closer to the true ellipticity curve rather than the H/V curve. To elaborate RayDec techniques consider a signal {where x(t) = e(t) or n(t) or v(t) }. These three time series has N number of data points and having length T. To obtain a Rayleigh wave ellipticity curve, the main idea of this method is to obtain only Rayleigh waves in comparison other waves type by the addition of a large number of filtered signal windows Δ, estimates the energy level of horizontal averaged and vertical signal in a location where the vertical component change its sign from -ve to +ve. Due to the phase shift of $\frac{\pi}{2}$ between Rayleigh wave vertical and horizontal component, both the horizontal component of EW and NS are projected by factor ϕ with north direction in such a way to maximized the correlation between the summed horizontal and vertical component. The Rayleigh wave ellipticity is obtained latterly from Eq.5 . The ellipticity E is calculated as the square root of the ratio of the energies in the signal window. Δ.

$$E = \sqrt{\frac{\int_0^\Delta hf^2.s(t)*dt,}{\int_0^\Delta vf^2.s(t)*dt}} \tag{5}$$

Natural Hazards
and Earth System
Sciences
Discussions

EGU
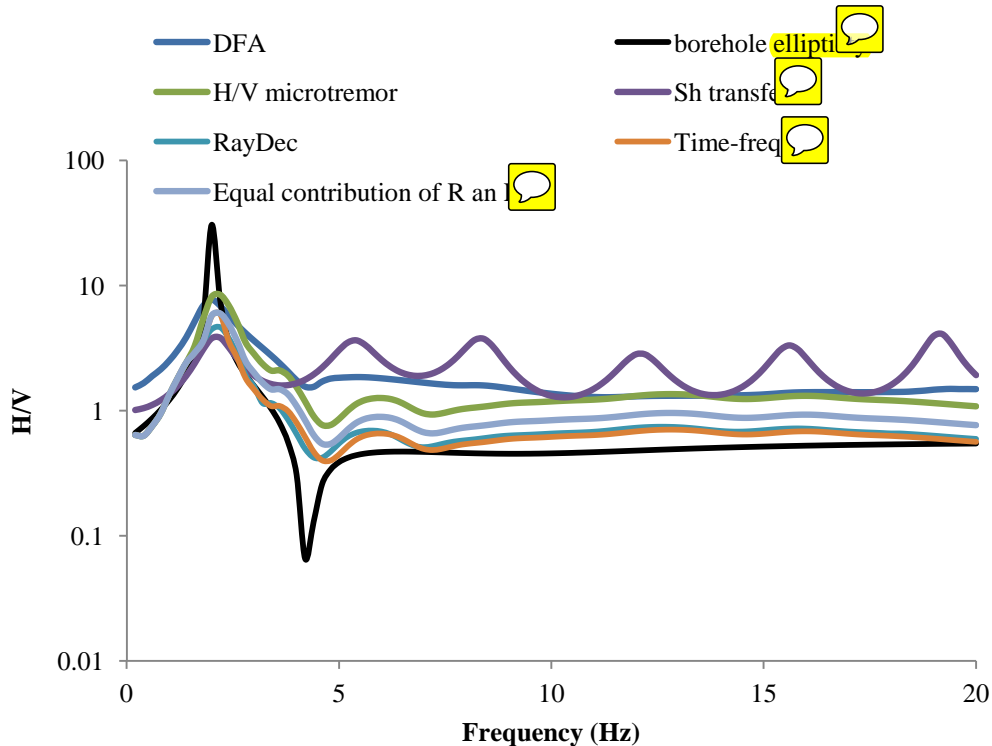
265 *where* hf.s (t) is the horizontal average (NS north-south , EW east-west) signal and Vf.s (t) is the

266 vertical component. This process is repeated for a whole record for an increment of window length Δ

267 .The window length is taken as function of frequency such that to ensure 10 significant cycle at chosen

268 frequency (Δ=10/f where f is the analyzing frequency from 0.2 to 20 Hz are used). There are two tuning

269 parameter for this technique , Δ (window length) and df (width of frequency filter). The effect of these

270 two tuning parameter on the result is shown Fig.9. For our analysis we used one-hour records of noise,

271 which were divided into 6 segments of 10 minutes each , afterward, the result is average out for all the

272 six segments with the aim for minimization of misfit (see for detail procedure Hobiger et al., 2009). The

273 result of ellipticity obtained via RayDec show a better match with borehole curve especially at right and

274 left limb.

275 The analysis of both time-frequency and RayDec for H/V give satisfactory result for the ellipticity

276 retrieval of Rayleigh waves. Fig 10 shows the comparison of all the technique retrieved curves with that

277 of borehole ellipticity.

278

Natural Hazards
and Earth System
Sciences

Open Access

Discussions

EGU

279
280

281 Fig.9 Ellipticity obtained via RADEL technique , (a) shows the effect signal duration on the result.(b) shows the effect of

282 using different width of window (c) shows the effect of different filter width on the result (d) shows six 10-minute windows

283 (ellipticity for each 10 minute is obtained at the end the result is average and compared with borehole data black line).

Natural Hazards
and Earth System
Sciences
Discussions

284
285   Fig.10 Show the comparison of borehole ellipticity curve combine with that of all elliptcity retrieval technique.

286 **7.Discussion and conclusion.**

287 Deep soil shear wave velocity information can be retrieved from the joint inversion of H/V curve with

288 dispersion curve. The H/V curve are assumed to be linked with Rayleigh wave ellipticity for a site.

289 However in real situation the H/V curve technique can not completely replicate the Rayleigh wave

290 ellipticity. It is because of the presence of different elastic wave influence presence in the H/V curve

291 retrieval. Diffuse field approach is a better way to consider the effect of all elastic seismic phases (body

292 and surface wave). However the analysis of our data shows that at singularities (peak and trough)

293 especially at peak of the H/V curve obtained via DFA is very well correlated with Rayleigh ellipticity

294 curve in term of these singularities frequency. This matching can be assumed that around the peak

295 frequency even in case of diffuse like field situation the seismic noise field is dominated surface wave

296 especially Rayleigh waves.

297 The other approach used for the H/V curve technique is linked to the surface wave dominancy

298 especially Rayleigh wave around the singularities. Three different polarization technique for retrieval of

16

Natural Hazards
and Earth System
Sciences
Discussions

Open Access

EGU

299 ellipticity curve by minimizing the SI. contribution to the horizontal component are simple H/V with

300 equal contribution of Rayleigh and Love wave, time-frequency analysis and RayDec technique. The

301 result of equal assumption of Rayleigh/Love wave fraction is unable to match with parts of borehole

302 ellipticity except at peak. However ellipticity curve retrieved from noise analysis through time-

303 frequency and RayDec shows a good replication of borehole ellipticity around the peak, right and left

304 limb.

305 For the deep soil deposit the joint inversion of ellipticity and dispersion curve of Rayleigh wave are

306 recommended. However due to the presence of effect of other seismic elastic phases especially Love

307 wave may produced some bias result. Therefore it is extremely necessary to retrieved a H/V curve

308 where the effect of Love wave contribution are minimized prior to the inversion with dispersion curve.

309 For our test site we found that time-frequency and RayDec show better result ,by replication left and

310 right limb of ellipticity curve of the borehole at the site.

319

320 **References:**

321 [1]. Aki, K., and P.G. Richards. : Quantitative seismology, Second Edition, University Science Books.**2002**

322 [2]. Arai, H., and K. Tokimatsu. : Evaluation of local site effects based on microtremor H/V spectra. Proceeding
323   of the Second International Symposium on he Effects of Surface Geology on Seismic Motion. Yokohama,
324   Japan.**2** 673-680, **1998.**

325 [3]. Bard, P.Y.: Microtremor measurements: a tool for site effect estimation?. The Effects of Surface Geology
326   on Seismic Motion, eds. K. Irikura, K. Kudo, H. Okada and T. Sasatani (Balkema, Rotterdam), 1251-1279,
327   **1999.**

328 [4]. Bonnefoy-Claudet, S., Cornou, C.,Bard, P.-Y., Cotton, F.,Moczo, P., Kristek, J. & F˙ah, D., 2006a. : H/V
329   ratio: a tool for site effects evaluation. Results from 1-D noise simulations, *Geophys. J. Int.,* 827–837, **2006.**

[5]. Bormann, P. NMSOP – New Manual of Seismological Observatory Practice. IASPEI. GeoForschungsZentrum Potsdam, Germany. **2002.**

[6]. Chouet, B., De Luca, G., Milana, G., Dawson, P., Martini, M., Scarpa, R. : Shallow velocity of Stromboli volcano, Italy, derived from small-aperture array measurements of Strombolian tremor. Bull. Seism. Soc. Am.**,** 88-3, 653-666,**1998**.

[7]. Cornou, C. Traitement d'antenne et imagerie sismique dans l'agglomération grenobloise (Alpes françaises): implications pour les effets de site (In french). Université Joseph Fourier**,**260 , **2002**.

[8]. D. Fäh, M . Wathelet, M. Kristekova, H. Havenith, B. Endrun, G. Stamm, V. Poggi, J. Burjanek, and C. Cornou. : Using ellipticity information for site characterisation. NERIES deliverable JRA4 D4. [Online]. Available: http://www.neries-eu.org , **2009**.

[9]. Endrun, B. : Love wave contribution to the ambient vibration H/V amplitude peak observed with array measurements, J. Seismol., 15**,** 443–472, **2011**.

[10]. Enrico Lunedei and Peter Malischewsky A. Ansal (ed.). : Perspectives on European Earthquake Engineering and Seismology, Geotechnical, Geological and Earthquake Engineering 39, DOI 10.1007/978-3-319-16964-4_15 , **2015**.

[11]. Hobiger, M., P.-Y. Bard, C. Cornou, and N. Le Bihan . : Single station determination of Rayleigh wave ellipticity by using the random decrement technique (RayDec), Geophys. Res. Lett., 36, L14303, doi:10.1029/2009GL038863, **2009**.

[12]. Horike, M. : Inversion of phase velocity of long period microtremors to the S-wave-velocity structure down to the basement in urbanized areas. J. Phys. Earth, 33, 59-96, **1985**.

[13].   Jorge Luís Porsani , Welitom Borges, Vagner Roberto Elis , Liliana Alcazar Diogo . : Investigações geofísicas de superfície e de poço no sítio controlado de geofísica rasa do IAGUSP, Revista Brasileira de Geofísica.**2004**.

[14]. Kohler, A., Ohrnberger, M. & Scherbaum, F. : The relative fraction of Rayleigh and Love waves in ambient vibration wavefields at different European sites, in Proceedings of the 3rd Int. Symp. on the Effects of *Surface Geology on SeismicMotion,* Grenoble, 30 August–01 September,Vol. 1, pp. 351–360, **2006**.

[15]. Konno, K., and T. Ohmachi . : Ground-Motion Characteristic Estimated from Spectral Ratio between Horizontal and Vertical Components of Microtremor. Bull. Seism. Soc. Am.,. 88, 228-241, **1998**.

[16]. Li, T. M. C., Ferguson, J. F., Herrin, E., D. H. B. : High-frequency seismic noise at Lajitas, Texas. Bull. Seism. Soc. Am. **74-5**, 2015-2033, **1984**.,.

[17]. M. Hobiger,, C. Cornou,1 M. Wathelet,G. Di Giulio,B. Knapmeyer Endrun, F. Renalier,P.-Y. Bard,1 A. Savvaidis, S. Hailemikael,N. Le Bihan,M. Ohrnberger and N. the Ground structure imaging by inversions of Rayleigh wave ellipticity sensitivity analysis and application to European strong-motion sites Geophys. J. Int.   192**,** 207–229.**2013**.

[18]. Mucciarelli M. and Gallipoli M.R. : *A* critical review of 10 years of microtremor HVSR technique. Boll. Geof.Teor. Appl., 42, 255-266, **2001**.

[19]. Okada, H. : The Microtremor Survey Method. Geophys. Monograph Series, SEG, 129 pp, **2003.**

[20]. Perton, M., S´anchez-Sesma, F.J., Rodr´ıguez-Castellanos, A., Campillo, M. & Weaver, R.L. : Two perspectives on equipartition in diffuse elastic fields in three dimensions, *J. acoust. Soc. Am.,* 126(3), 1125–1130, **2009**.

[21]. Picozzi, M., Parolai, S., Richwalski, S.M. : Joint inversion of H/V ratios and dispersion curves from seismic noise: Estimating the S-wave velocity of bedrock. Geoph. Res. Lett., 32, No.11doi: 10.1029/2005GL022878

[22]. Sanchez-Sesma, F.J. : A theory for microtremor H/V spectral ratio: application for a layered medium, *Geophys. J. Int.,* **2011**, **186**(1), 221–225, **2005**.

375   [23]. Scherbaum, F., K.-G. Hinzen, and M. Ohrnberger,. : Determination of shallow shear-wave velocity
376   profiles in Cologne, Germany area using ambient vibrations. Geophys. J. Int. 152, 597-612, **2003**.
377   [24]. SESAME scientific products at http://SESAME.geopsy.org/SES_Reports.htm., **2001-2004**
378   [25]. Tokimatsu, K. : Geotechnical site characterization using surface waves. Earthquake Geotechnical
379   Engineering, Ishihara (ed.), Balkema, Rotterdam, 1333-1368, **1997**.
380   [26]. Yamamoto, H. (2000). : Estimation of shallow S-wave velocity structures from phase velocities of love-
381   and Rayleigh- waves in microtremors. Proceedings of the 12th World Conference on Earthquake
382   Engineering. Auckland, New Zealand, **2000.**
383   [27]. Yamanaka, H., Takemura, M., Ishida, H, Niwa, M. : Characteristics of long-period microtremors and their
384   applicability in exploration of deep sedimentary layers. Bull. Seism. Soc. Am. 84, 1831-1841, **1994**.

385